Available online at www.sciencedirect.com
ScienceDirect
Journal of Sound and Vibration 311 (2008) 224–242
JOURNAL OF SOUND AND VIBRATION
www.elsevier.com/locate/jsvi

Active control of radiated pressure of a submarine hull

Xia Pan*, Yan Tso, Ross Juniper

Maritime Platforms Division, Defence Science and Technology Organisation, P.O. Box 4331, Melbourne, Victoria 3001, Australia

Received 26 July 2006; received in revised form 23 August 2007; accepted 2 September 2007
Available online 22 October 2007

Abstract

A theoretical analysis of the active control of low-frequency radiated pressure from submarine hulls is presented. Two typical hull models are examined in this paper. Each model consists of a water-loaded cylindrical shell with a hemispherical shell at one end and conical shell at the other end, which forms a simple model of a submarine hull. The conical end is excited by an axial force to simulate propeller excitations while the other end is free. The control action is implemented through a Tee-sectioned circumferential stiffener driven by pairs of PZT stack actuators. These actuators are located under the flange of the stiffener and driven out of phase to produce a control moment. A number of cost functions for minimizing the radiated pressure are examined. In general, it was found that the control system was capable of reducing more than half of the total radiated pressure from each of the submarine hull for the first three axial modes.

1. Introduction

The work described in this paper is concerned with the active control of sound pressure radiation of submarine hulls subjected to an axial force to simulate propeller excitations.

The radiated pressure of a finite cylindrical shell in axisymmetric vibration has been investigated by Tso and Jenkins [1]. In their study, they simulated the response of a submarine hull due to propeller excitations as a water-loaded finite cylinder subjected to an axial force. Their model is developed for low-frequency applications such as blade tonal noise. The active control of vibration transmission in a cylindrical shell has been studied by Pan and Hansen [2,3] using circumferential arrays of vibration control actuators and sensors. Young [4] studied the active control of vibration of an air duct using an angled stiffener and point forces. Tso, Kessissoglou and Norwood [5,6] carried out an analysis of the active control of the first two structural modes of a cylindrical shell using an axial force applied at the opposite end of a primary excitation source. However, the amplitude of the axial force required was about the same order as the primary excitation, making this method impractical for real maritime applications.

Recently, Pan et al. [7] developed a control strategy for a large submerged finite cylinder by using a Tee-sectioned circumferential stiffener and pairs of PZT stack actuators driven out of phase to produce control moments around the circumference of the cylindrical shell (see Fig. 1). They demonstrated that the

*Corresponding author. Tel.: +61 39626 8283; fax: +61 39626 8373.
E-mail address: xia.pan@dsto.defence.gov.au (X. Pan).

0022-460X/$ - see front matter
doi:10.1016/j.jsv.2007.09.001

Nomenclature

a	hull radius
c_f	speed of sound in the fluid
E	Young's modulus
F	primary force amplitude
G	$= E_{\text{hem}}h_{\text{hem}}/a^2(1-v_{\text{hem}}^2)$
h	shell thickness
h_n	spherical Hankel function of order n
H_n	Hankel function of order n
j	$\sqrt{-1}$
j_n	spherical Bessel function of order n
J_n	Bessel function of order n
k_f	$= f/c_f$ wavenumber of fluid
k_{con}	$\sqrt{\rho_{\text{con}}\omega^2(1-v_{\text{con}}^2)/E_{\text{con}}h_{\text{con}}}$
L	length of cylindrical shell
l	length of conical shell
M	control moment amplitude
n	order number
P	sound power
P_n	Legendre functions of order n
p	sound pressure
r	radius of conical shell at distance $x(r = a + x\tan\alpha)$
R	distance from middle section of pressure hull to the observer
s	$= \cos\theta_{\text{hem}}$
u	axial displacement
w	radial displacement
α	half-cone angle
v	Poisson ratio
ρ_f	density of fluid
θ	angle between the axis of pressure hull and the line connecting the middle section of pressure hull to the observer
σ_n	$= n(n+1)$
ω	angular frequency
$\|\ \|$	vector amplitude

Superscripts

$'$	derivative
*	complex conjugate

Subscripts

c	cylindrical shell
con	conical shell
f	fluid
hem	hemispherical shell
c-f	cylindrical shell response due to unit primary force
c-m	cylindrical shell response due to unit control moment
con-f	conical shell response due to unit primary force
con-m	conical shell response due to unit control moment
hem-f	hemispherical shell response due to unit primary force
hem-m	hemispherical shell response due to unit control moment
tot	total value

control system was capable of producing control moments of sufficient amplitude to reduce the total radiated pressure from the cylinder. A comparison of the analytical model [7] and a coupled FE/BE model on the dynamic response and structurally radiated sound pressure of a submarine hull under an axial excitation has

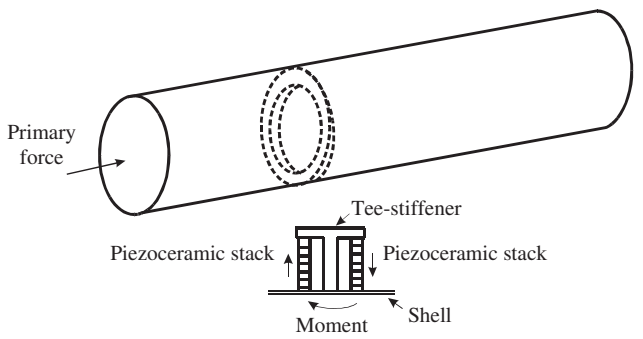

Fig. 1. Pressure hull showing primary force, control actuators and T-stiffener.

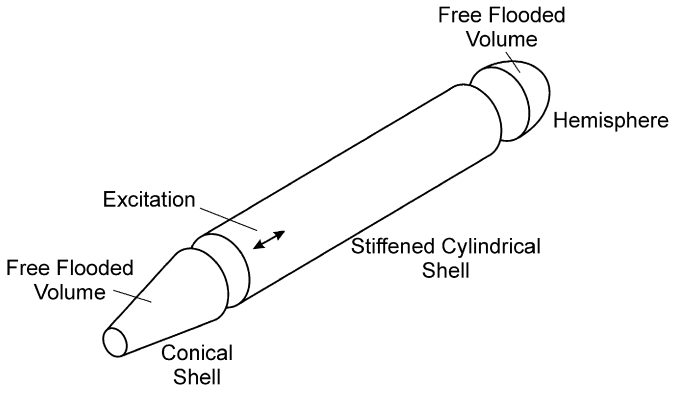

Fig. 2. A simplified submarine hull with conical, cylindrical and hemispherical shells.

been conducted in a parallel study [8]. The comparison shows good agreement between the two models for the first three axial modes. However, Tso and Jenkins [1] indicated that the asymmetry between the fore and aft end structures of a submarine hull could have a significant impact on both the level and directivity of the radiated noise. A modification to the cylinder model [7] is therefore required to include the fore and aft casings in order to predict the hull response and sound radiation of a submarine.

The work outlined in this paper investigates the application of a novel control technique [7] to a simplified submarine hull model (see Fig. 2) which consists of a cylindrical shell with end casings [1]. Feed forward active control strategy is used in the analysis. With this control strategy, the combination of the stiffener and the actuators are capable of developing a control moment of sufficient amplitude to reduce the total radiated pressure from the submarine hull at low frequencies.

The present analysis assumed that the axial force is the dominant cause of underwater radiated noise at the low frequencies of interest. The effects of propeller moments and forces in other directions, and of forces transmitted through the fluid to external hull surfaces [9], are not included in this analysis.

2. Axisymmetric response of the submarine hull

This section describes a low-frequency model for the axisymmetric vibration of a pressure hull with free-flooded casings attached to both ends. The pressure hull is modelled as a finite cylindrical shell with circumferential ring stiffeners and rigid end plates. The end conditions of the cylindrical shell are matched with those of the end casings which are modelled as hemispherical and conical shells. For the example pressure hull structures considered in this paper, these end conditions are zero radial displacement and slope at both ends of the pressure hull. Additionally, the fore end of the pressure hull is free while the aft end is subjected to an axial force due to propeller excitations.

The dynamic analysis of a finite cylinder with different end conditions has been considered by many authors and therefore it will not be repeated here. The readers may refer to Refs. [10,11] for a detailed study.

2.1. Modelling of the fore casing

The fore casing of a submarine normally consists of a free-flooded enclosure which loosely resembles the shape of a hemispherical shell. The edge of the shell is subjected to a tangential displacement due to the axial motion of the pressure hull (see Fig. 3). It is assumed that, due to the free-flooded nature of the casing, the structure would be more flexible compared with the pressure hull and therefore the bending stiffness of the shell may be ignored. This results in a set of membrane equations for the solution of shell response.

The equation of motion for a fluid loaded hemispherical shell in axisymmetric motion, with the assumption that the bending stiffness of the shell is negligible, may be expressed in terms of the Legendre

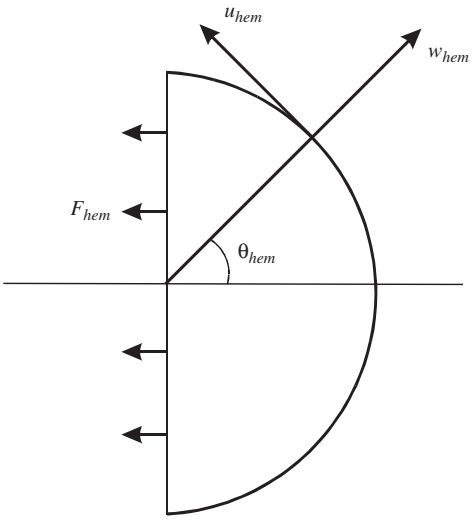

Fig. 3. A hemispherical shell showing input line force and displacements.

function $P_{n+1}(s)$ $(n = 1,3,5\ldots)$ [1]:

$$\begin{bmatrix} a_{11} & a_{12} \\ a_{21} & a_{22} + \mathrm{FL} \end{bmatrix} \begin{bmatrix} u_n \\ w_n \end{bmatrix} = \begin{bmatrix} -\dfrac{|F_{\mathrm{hem}}|}{\mathrm{an}}(2n+1)P_{n+1}(0) \\ 0 \end{bmatrix}, \tag{1}$$

where $a_{11} = \mathrm{G}(v_{\mathrm{hem}} + \sigma_n - 1) - \omega^2 \rho_{\mathrm{hem}} h_{\mathrm{hem}}$, $a_{21} = \sigma_n a_{12}$, $a_{22} = 2G(1 + v_{\mathrm{hem}}) - \omega^2 \rho_{\mathrm{hem}} h_{\mathrm{hem}}$, u_n, v_n are the spectral displacements of the shell, $|F_{\mathrm{hem}}|$ is the amplitude of the line force in N/m, the fluid loading term FL is giving by

$$\mathrm{FL} = \omega \rho_f c_f \left[\frac{h_n(k_f a)}{h_n'(k_f a)} - \frac{j_n(k_f a)}{j_n'(k_f a)} \right].$$

The tangential displacement u_{hem} and the radial displacement w_{hem} for a hemispherical shell, with the boundary condition of no radial displacement at the edge, may be expressed in terms of the Legendre function $P_n(s)$ $(n = 1,3,5\ldots)$ [12]:

$$u_{\mathrm{hem}} = \sum_{n=1,3,5}^{\infty} u_n (1 - s^2)^{1/2} \frac{\mathrm{d}P_n(s)}{\mathrm{d}s} \tag{2}$$

and

$$w_{\mathrm{hem}} = \sum_{n=1,3,5}^{\infty} w_n P_n(s). \tag{3}$$

In order to satisfy the boundary conditions of the hemispherical shell, the amplitude of the line force is chosen such that the tangential displacement at the edge of the shell matches the axial displacement at the fore end plate of the cylinder.

2.2. Modelling of the aft conical shell

To investigate the structural response and noise radiation at the aft section of a submarine hull due to an axial excitation, the aft hull structure may be modelled as a truncated conical shell with fluid loading on both sides. For the purpose of this analysis, it is assumed that the conical shell structure has a small cone angle so that the method of small perturbations [13] may be applied.

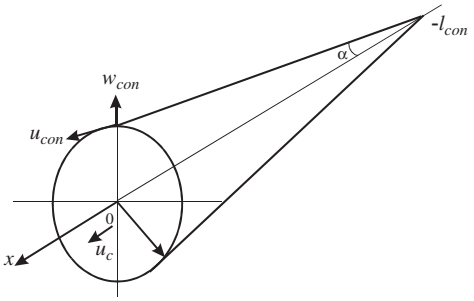

Fig. 4. Coordinate system of conical shell.

Consider the case where a conical shell (refer to Fig. 4) of length l is subjected to an axial displacement of u_c at $x = 0$ and free at the other end ($x = -l_{\text{con}}$). The system equations due to the boundary conditions, which describe the amplitudes of the conical shell, lead to

$$u_{\text{con}} \cos \alpha - w_{\text{con}} \sin \alpha = u_c \tag{4.1}$$

and

$$-\frac{E_{\text{con}} h_{\text{con}}}{(1-\upsilon_{\text{con}}^2)}\left[\cos \alpha \frac{\mathrm{d}u_{\text{con}}}{\mathrm{d}x} + \frac{\upsilon_{\text{con}}}{r}(u_{\text{con}} \sin \alpha + w_{\text{con}} \cos \alpha)\right] = 0. \tag{4.2}$$

Using the method of small perturbations, the meridian displacement u_{con} and the radial displacement w_{con} of the cone are given by Tso and Jenkins [1]:

$$u_{\text{con}} = \sum_{i=1}^{2} A_i r^{-1/\upsilon_{\text{con}}} \mathrm{e}^{-\mathrm{j}\eta_i} \tag{5}$$

and

$$w_{\text{con}} = \sum_{i=1}^{2} A_i R_i r^{-1/\upsilon_{\text{con}}} \mathrm{e}^{-\mathrm{j}\eta_i}, \tag{6}$$

where

$$\eta_{1,2} = \int_0^x \frac{\xi_{1,2}}{r}\,\mathrm{d}z,$$

$$R_{1,2} = -\mathrm{j}\left(\frac{k_{\text{con}}^2 r^2 - \xi_{1,2}^2}{\xi_{1,2}\upsilon_{\text{con}}}\right).$$

ξ_1 and ξ_2 are the roots of the conical characteristic equation. The amplitudes A_1 and A_2 may be determined by substituting Eqs. (5) and (6) into Eqs. (4.1) and (4.2).

3. Total sound radiation from the submarine hull

The total pressure radiated by the submarine hull model is obtained by combining the components of radiated pressure due to the cylindrical shell and the end casings, with the appropriate phasing considered for each of the components. This may be achieved by referring the radiated pressure of the pressure hull and end casings to the mid-section of the cylindrical shell.

The contribution to total radiated pressure due to the radial motion of the cylinder may be obtain from the Helmholtz integral equation [10] and Appendices A and B give the radiated sound pressure for the hemispherical shell and conical shell, respectively.

4. Active control of total sound radiation

As a first approximation, the control action due to the stiffener and the stack actuators is replaced by a circumferential line moment acting around a bulkhead as reported in Ref. [7]. The inclusion of the bulkhead demonstrates how the method of analysis may be applied to shells with structural discontinuities. A simplified model of the pressure hull may then be considered as a structural junction with two cylindrical shells and a circular plate.

At any location (R,θ), the pressure due to the radial motion of the cylindrical shell for the primary and control excitation is given by Pan et al. [7]:

$$p_c(R,\theta) = Fp_{c\text{-}f}(R,\theta) + Mp_{c\text{-}m}(R,\theta). \tag{7}$$

The pressure due to the hemispherical shell may be expressed as

$$p_{\text{hem}}(R,\theta) = Fp_{\text{hem}\text{-}f}(R,\theta) + Mp_{\text{hem}\text{-}m}(R,\theta). \tag{8}$$

Similarly, the pressure due to the conical shell is given by

$$p_{\text{con}}(R,\theta) = Fp_{\text{con}\text{-}f}(R,\theta) + Mp_{\text{con}\text{-}m}(R,\theta). \tag{9}$$

The total sound radiation is defined as the amplitude of the sum of the three components and may be expressed as

$$p_{\text{tot}}(R,\theta) = \left|p_c(R,\theta) + p_{\text{hem}}(R,\theta) + p_{\text{con}}(R,\theta)\right|. \tag{10}$$

To obtain the optimal control moment, the radiated sound power is chosen as the cost function for minimization. Eq. (11) below gives the expression for sound power:

$$P = \frac{2\pi R^2}{\rho_f c_f}\int_0^{\pi} |p_c(R,\theta) + p_{\text{hem}}(R,\theta) + p_{\text{con}}(R,\theta)|^2 \sin\,\theta\,\mathrm{d}\theta. \tag{11}$$

The optimal control moment may then be obtained by evaluating the derivative of Eq. (11) with respect to the control moment and setting the results to zero:

$$M = -F\frac{\int_0^{\pi}[p_{c\text{-}f}(R,\theta) + p_{\text{hem}\text{-}f}(R,\theta) + p_{\text{con}\text{-}f}(R,\theta)][p_{c\text{-}m}(R,\theta) + p_{\text{hem}\text{-}m}(R,\theta) + p_{\text{con}\text{-}m}(R,\theta)]^*\,\mathrm{d}\theta}{\int_0^{\pi}|p_{c\text{-}m}(R,\theta) + p_{\text{hem}\text{-}m}(R,\theta) + p_{\text{con}\text{-}m}(R,\theta)|^2\,\mathrm{d}\theta}. \tag{12}$$

An optimal control moment which minimizes a different cost function is shown in Ref. [7].

The selection of control actuator locations was based on an earlier analysis [7], where the control actuators were located near the ends of the cylinder for maximum control effect.

5. Numerical results

Two submarine models with different pressure hull diameters were considered in this section for comparison. Tables 1 and 3 show the parameters of the two models. In general, the shell parameters for the large submarine hull are scaled-up by a factor of approximately 1.3 from the small submarine hull except for

Table 1
Shell parameters of the small diameter submarine

Parameter	Value
Hull radius a	3.5 m
Hull length L	60.0 m
Hull thickness h_c	0.025 m
Hemispherical shell thickness h_{hem}	0.014 m
Conical shell length l	11.0 m
Conical shell thickness h_{con}	0.014 m
Half-cone angle α	18°

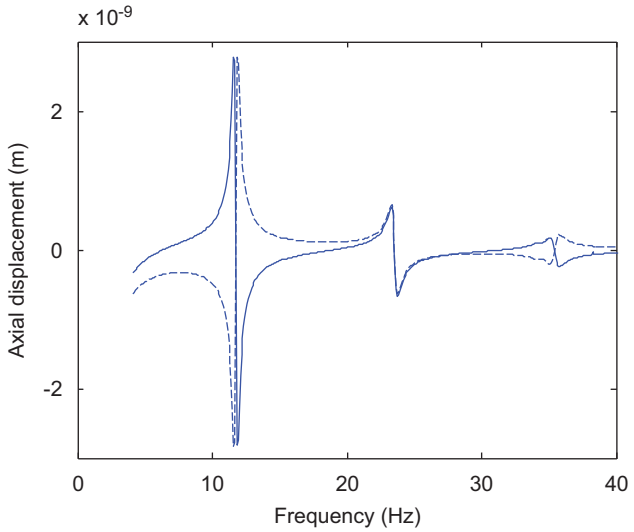

Fig. 5. Axial response of small diameter hull. —, axial displacement at $x = 0$, - - -, axial displacement at $x = L$.

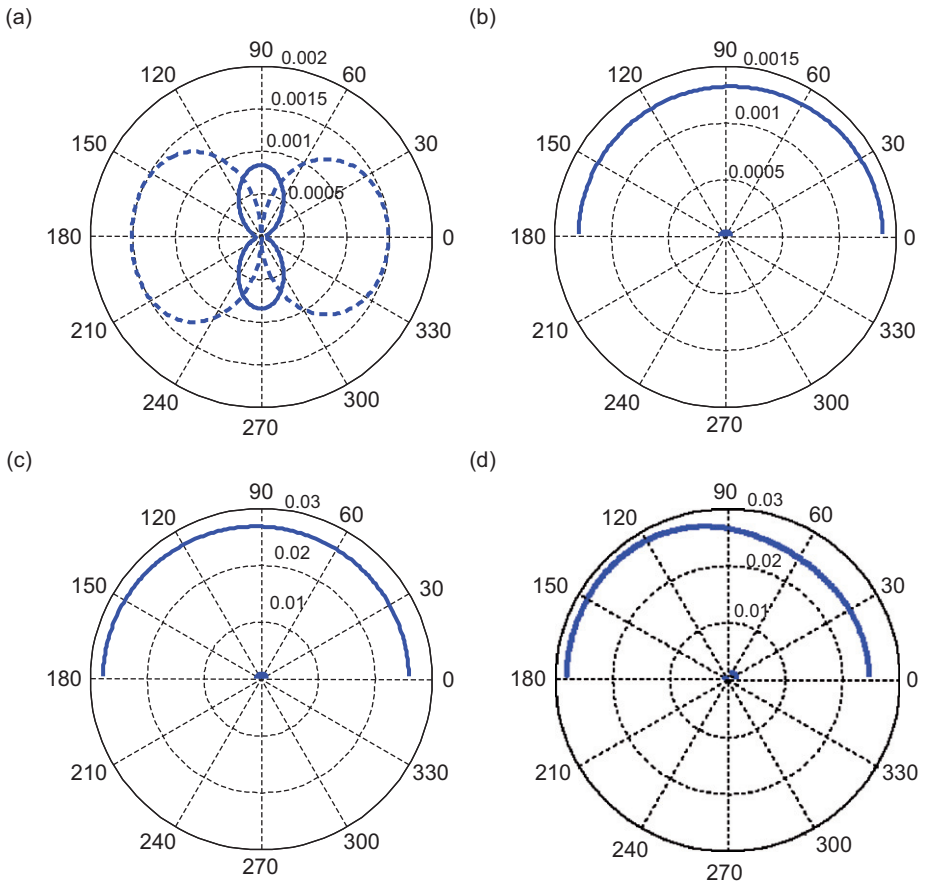

Fig. 6. Radiated pressure of small diameter hull at first axial mode by minimizing cylinder sound power. In this and all other figures except Fig. 9, the radiated pressure is plotted in polar coordinate with angle in degrees and radius in Pascals: (a) due to cylindrical shell; (b) due to hemispherical shell; (c) due to conical shell; (d) total radiated pressure. —, uncontrolled; - - -, controlled.

the spacing of ring stiffeners which is the same for both models. Also, distributed mass is added to the pressure hull to give a reserve of buoyancy of approximately 12% for both submarine models (as is the case for modern submarine design) and the lumped masses at the front and rear of the pressure hull are adjusted to maintain a condition of neutral buoyancy to simulate the function of the main ballast tanks. The cylindrical, hemispherical and conical shells are made of steel of different thickness as shown in Tables 1 and 3.

The results presented in this section were based on a primary excitation force in the axial direction of 1 N amplitude applied to the pressure hull at $x = 0$. The sound pressure level at a distance of 1000 m was used as a reference signal for comparison. It also acted as an error signal for sound radiation control. As discussed in Section 4, the cost function to be minimized is the total radiated sound power from the pressure hull, which consists of the cylindrical shell and the rigid end plates. This method of control may be implemented by an array of accelerometers to measure the radial motion of the cylindrical shell to determine the radiated pressure from the cylinder (refer to the acceleration measurement system in Ref. [4]), as well as measurement of the axial acceleration of the end plates.

Table 2
Line moment location and moment/force ratio for the small diameter

Axial mode	Location of moment (m)	Moment/force ratio
First mode	59.75	0.36
Second mode	0.25	0.12
Third mode	0.25	0.007

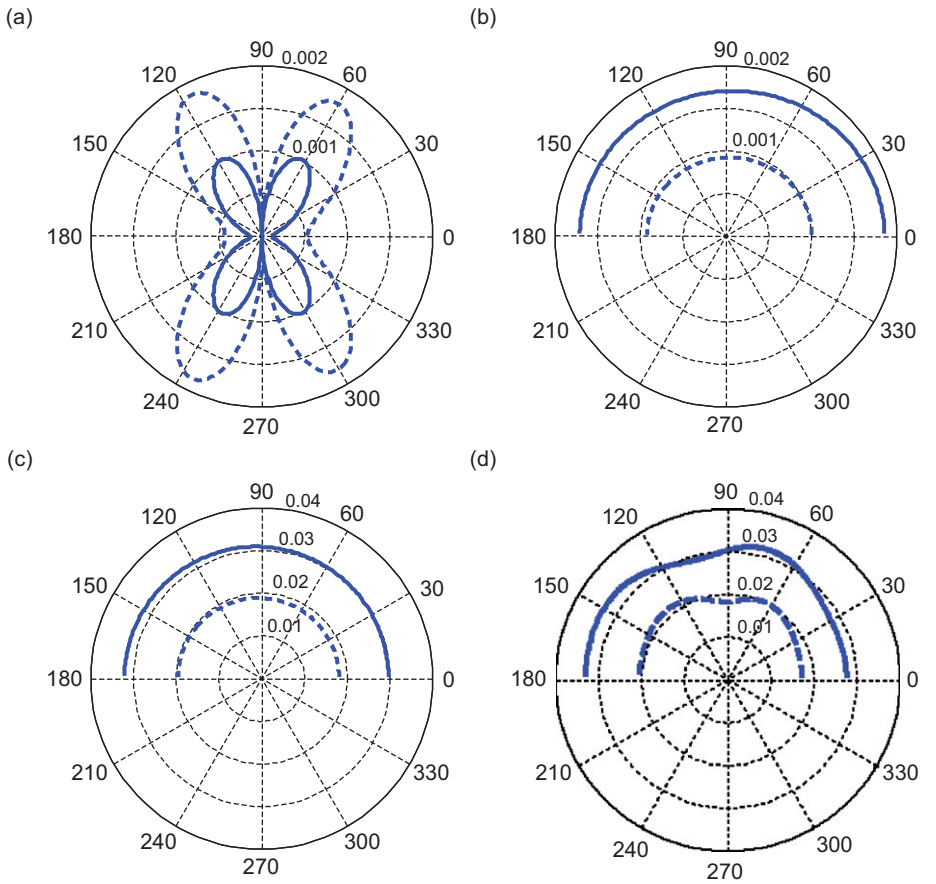

Fig. 7. Radiated pressure of small diameter hull at second axial mode by minimizing cylinder sound power.

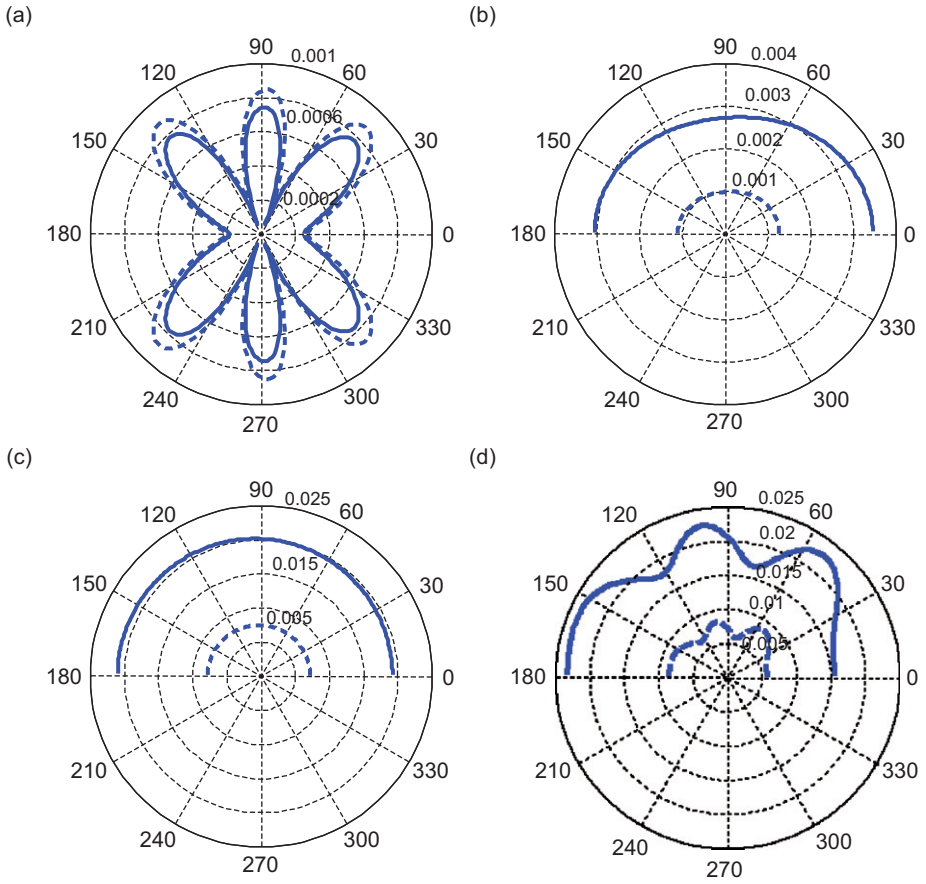

Fig. 8. Radiated pressure of small diameter hull at third axial mode by minimizing cylinder sound power.

Table 3
Shell parameters of the large diameter submarine

Parameter	Value
Hull radius a	4.6 m
Hull length L	79.0 m
Hull thickness h_c	0.033 m
Hemispherical shell thickness h_{hem}	0.018 m
Conical shell length l	14.0 m
Conical shell thickness h_{con}	0.018 m
Half-cone angle α	18°

In order to obtain a realistic amplitude near the resonant frequency of the hull, a structural loss factor of 0.02 was used in the calculations. It is assumed that the pressure hull is in axisymmetric vibration. Therefore, the only circumferential mode considered here is the breathing mode. For the purpose of this study, the results presented here are for the first three axial modes.

5.1. Results for the small diameter hull

Fig. 5 shows the axial displacement at both ends of the pressure hull as a function of frequency. It can be seen that the first three axial modes occur at frequencies of approximately 12, 24 and 35 Hz. The parameters of the submarine hull model are listed in Table 1 below.

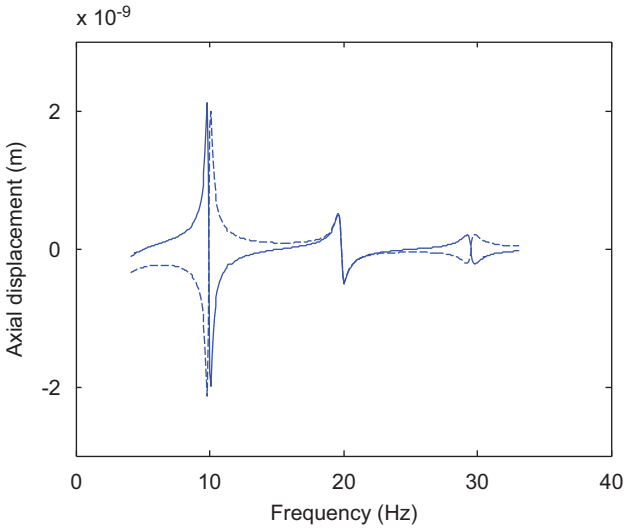

Fig. 9. Axial response of large diameter hull. —, axial displacement at $x = 0$, - - -, axial displacement at $x = L$.

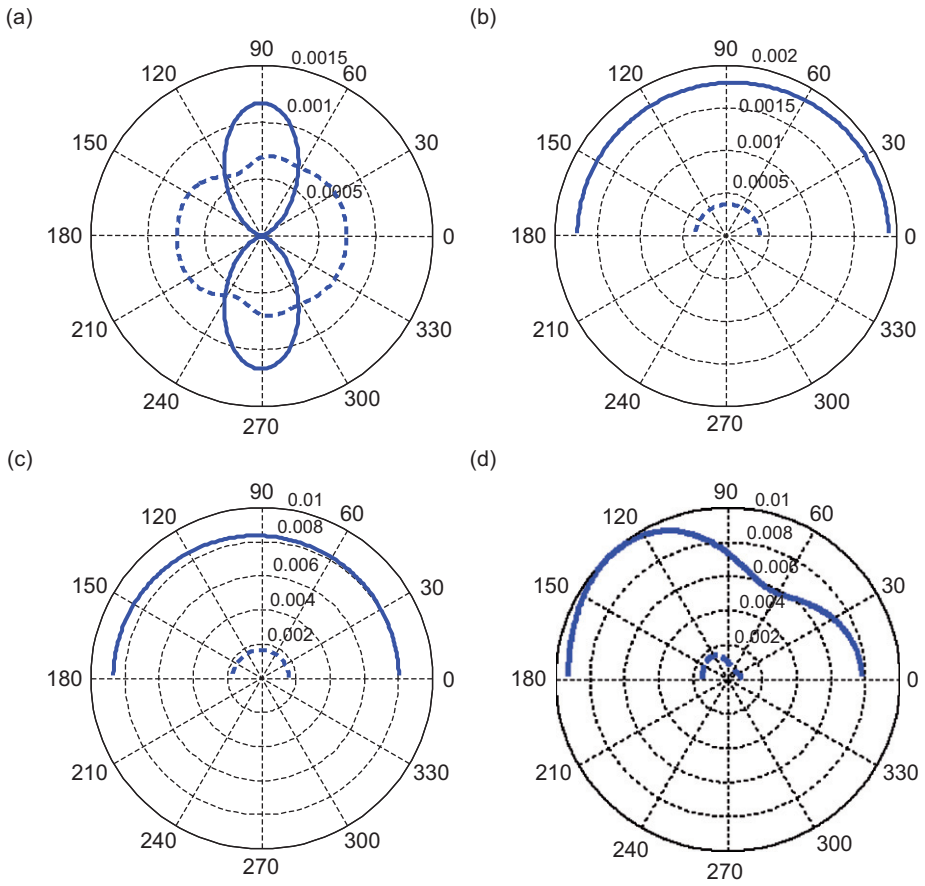

Fig. 10. Radiated pressure of large diameter hull at first axial mode by minimizing cylinder sound power.

5.1.1. Radiation at first mode

Fig. 6(a) shows the controlled and uncontrolled radiated pressure due to the radial motion of the cylindrical shell at the first axial mode. It can be seen that the control action has changed the pattern of the radiated pressure due to the location of the control actuators which is situated at approximately the free end of the pressure hull (see Table 2). This resulted in the generation of pressure fields at the cylinder ends. Also, the amplitude of the radiated pressure of the cylindrical shell has increased as a result of the control action.

Figs. 6(b and c) show the results for the hemispherical and conical shells, respectively. In both cases, the radiated pressure with control actions is insignificant compared with the uncontrolled radiated pressure. Numerical results reveal that the control action has achieved approximately 95% reduction of the radiated pressure for both the hemispherical and conical shells.

By comparing the results shown in Figs. 6(a–c), it can be observed that the radiated pressure is dominated by the conical shell due to its unconstrained end condition. This results in a large radial displacement and thus a high contribution of the total radiated pressure. Therefore, a large reduction in the radiated pressure of the conical shell results in a reduction of 90% of the total radiated pressure (see Fig. 6(d)), even if the control action increases the radiated pressure of the cylindrical shell (see Fig. 6(a)).

5.1.2. Radiation at higher axial modes

Figs. 7 and 8 show the results of radiated pressure at the second and third modes, respectively. It can be seen that the effects of the control action broadly follow the same pattern as for the first axial mode, except that the reduction in total radiated pressure in these cases are only about 40% and 65% for the second and third mode, respectively.

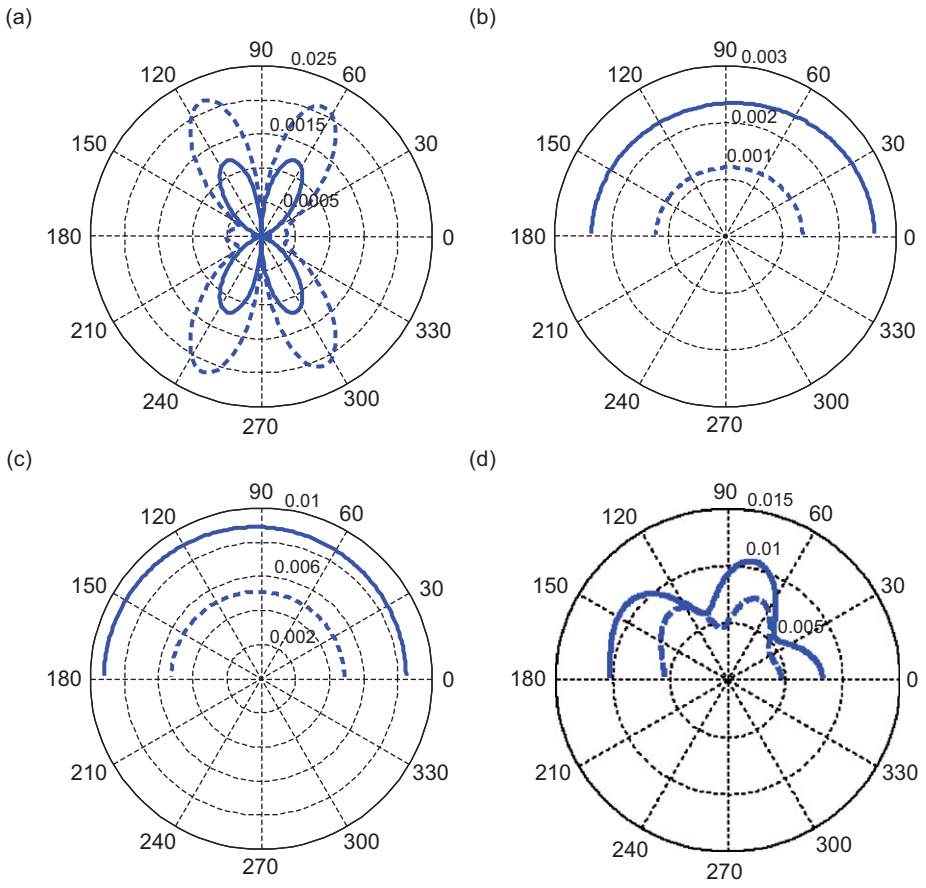

Fig. 11. Radiated pressure of large diameter hull at second axial mode by minimizing cylinder sound power.

The locations of the control moment and the ratio between the amplitude of control moment (defined as moment per unit length, Nm/m) and the primary force (N) are shown in Table 2. It can be seen that the amplitude of the control moment is about one-third of the primary force for the first mode and much lower for the higher modes. Therefore, at high order modes, the control performance is more efficient for this control configuration.

5.2. Results for the large diameter hull

The shell parameters for this submarine hull model are scaled-up by a factor of approximately 1.3 from the previous model and listed in Table 3 below:

Fig. 9 shows the axial displacement at both ends of the pressure hull as a function of frequency. As expected, the first three axial modes are slightly lower than those of the small diameter hull at 10, 20 and 29 Hz.

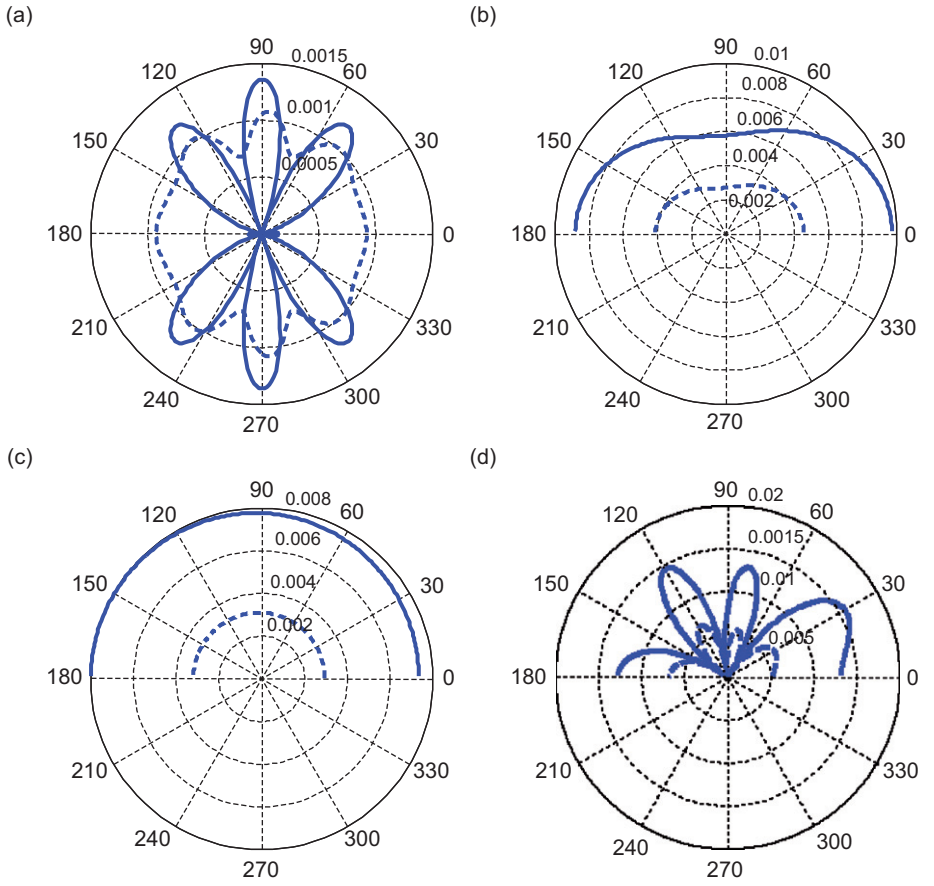

Fig. 12. Radiated pressure of large diameter hull at third axial mode by minimizing cylinder sound power.

Table 4
Line moment location and moment/force ratio for the large diameter

Axial mode	Location of moment (m)	Moment/force ratio
First mode	78.27	0.14
Second mode	0.32	0.10
Third mode	78.27	0.04

Figs. 10, 11 and 12 show the results of the first three axial modes for the large diameter submarine hull. It can be seen that the results are similar to those shown in Figs. 6, 7 and 8 for the smaller diameter hull, with a reduction in radiated pressure of 80%, 40% and 60% for the first, second and third mode, respectively. The small difference in radiation pattern between the two models might have been caused by the difference in the wavelength of sound to hull diameter ratio for the two models, given that their resonant frequencies are not in inverse proportional to hull dimensions, whereas the wavelength of sound is inversely proportion to the frequency. Thus the wavelength of sound to hull diameter ratio is not the same for the two models at a particular resonance. Also, there are some subtle differences in the scaling factor such as the spacing between the stiffeners, the magnitude of the distributed mass and the magnitude of the lumped masses, as discussed earlier at the beginning of Section 5.

Table 4 shows the locations of the control actuator and the amplitude ratio between the control moment and primary force. Again, the amplitudes of the control moments are much lower than the primary force, particularly for the higher modes.

5.3. *Effect of cost functions*

In the previous sections, the cost function to be minimized is the total radiated sound power from the pressure hull which consists of the cylindrical shell and the rigid end plates. Referring back to the results for the radiated pressure of the submarine hull model, it can be seen that the major contributor to the radiated noise is the conical shell which is subjected to an axial excitation. It is therefore interesting to include in this

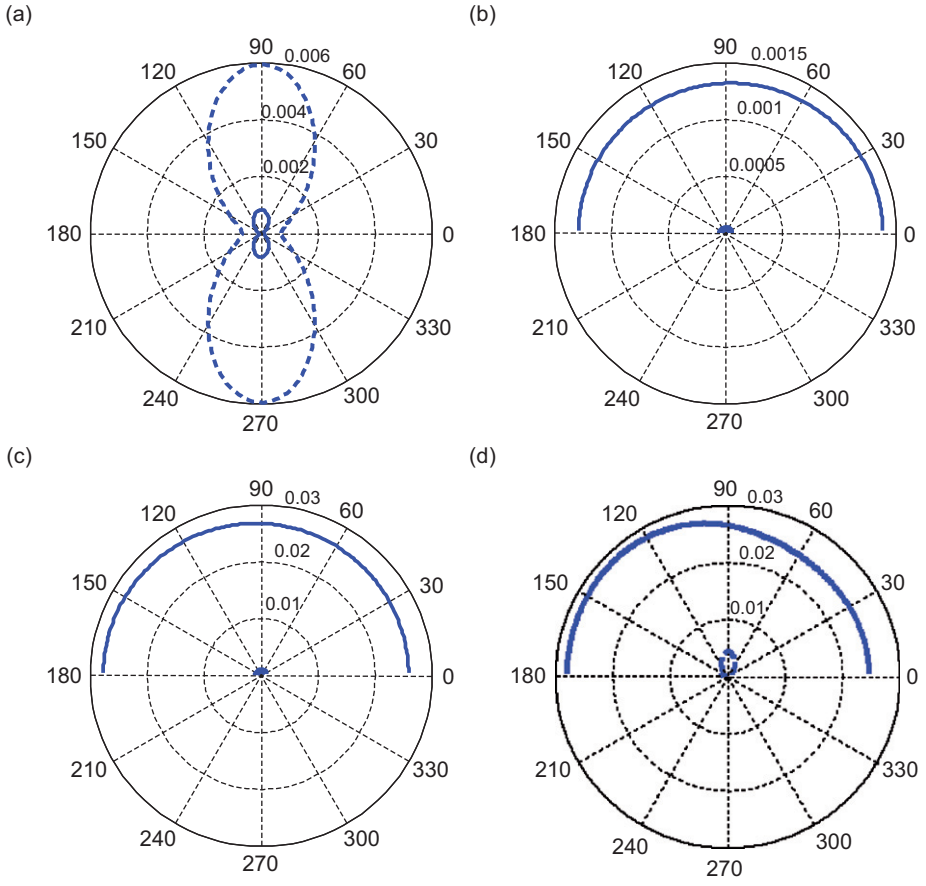

Fig. 13. Radiated pressure of small diameter hull at first axial mode by minimizing the sum of the axial displacement of the rigid end plates.

section an investigation using the sum of the axial displacement of the end plates as the cost function for minimization. In addition, results using the total radiated sound power of the submarine hull (cylindrical shell with the free-flooded end casings) as the cost function are also presented for comparison. Only the results for the first axial mode of the two submarine hull models are presented here to illustrate the effect of using different cost functions on reducing the radiated pressure.

Figs. 13 and 14 show results of the small diameter hull using the axial displacement and hull radiated sound power as the cost function, respectively. It can be seen that both the radiated sound power from the hull (Fig. 14) and the cylinder (Fig. 6) may be used effectively as the cost function with a reduction in radiated pressure of approximately 90%. The use of axial displacement as the cost function resulted in a small broadside radiation (see Fig. 13).

Similarly, results for the large diameter hull model are shown in Figs. 15 and 16. In general, the results follow the same pattern as for the small diameter hull model, with the axial displacement cost function showing a higher broadside radiation (see Fig. 15) compared with the small diameter hull model. Also, the hull radiated sound power cost function shows a slightly more significant radiated pressure reduction compared with the cylinder radiated sound power cost function (see Figs. 10 and 16).

5.4. *Effect of end conditions of the aft casing on radiated pressure*

In the previous sections, the conical shell is subject to an axial displacement at $x = 0$ and free at the other end ($x = -l_{\mathrm{con}}$). In this section, a radial constraint at $x = -l_{\mathrm{con}}$ is examined. The constraint equation is given by

$$w_{\mathrm{con}} = 0. \tag{4.3}$$

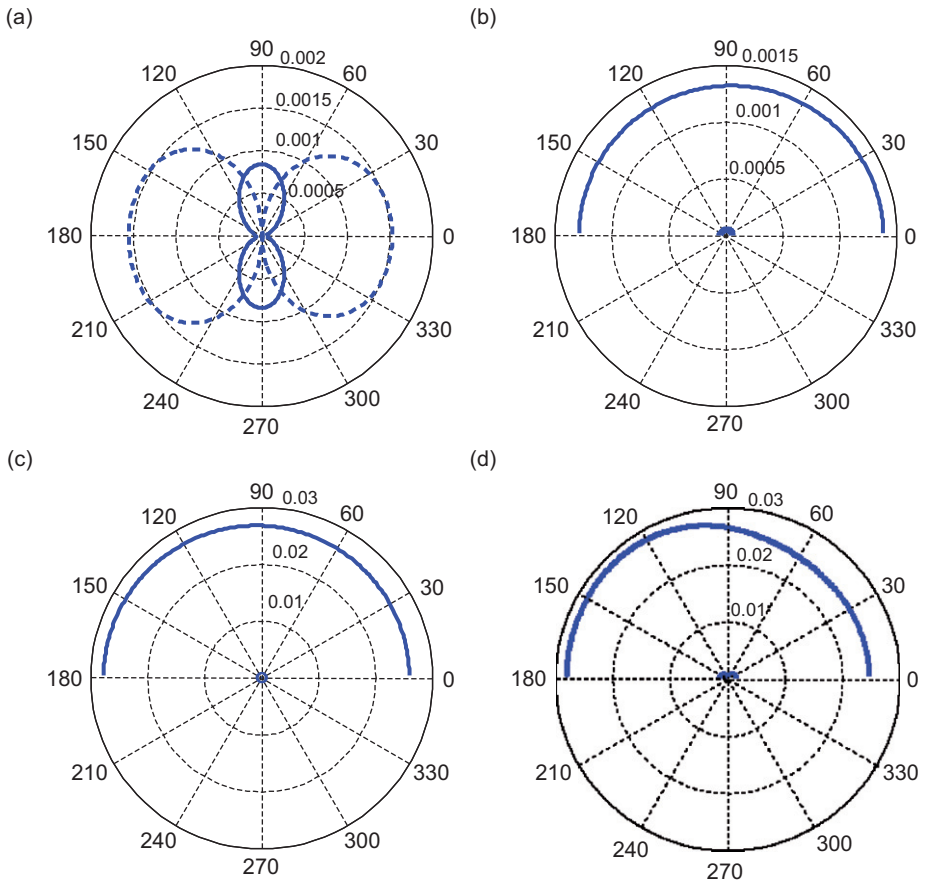

Fig. 14. Radiated pressure of small diameter hull at first axial mode by minimizing the total radiated sound power of the submarine hull.

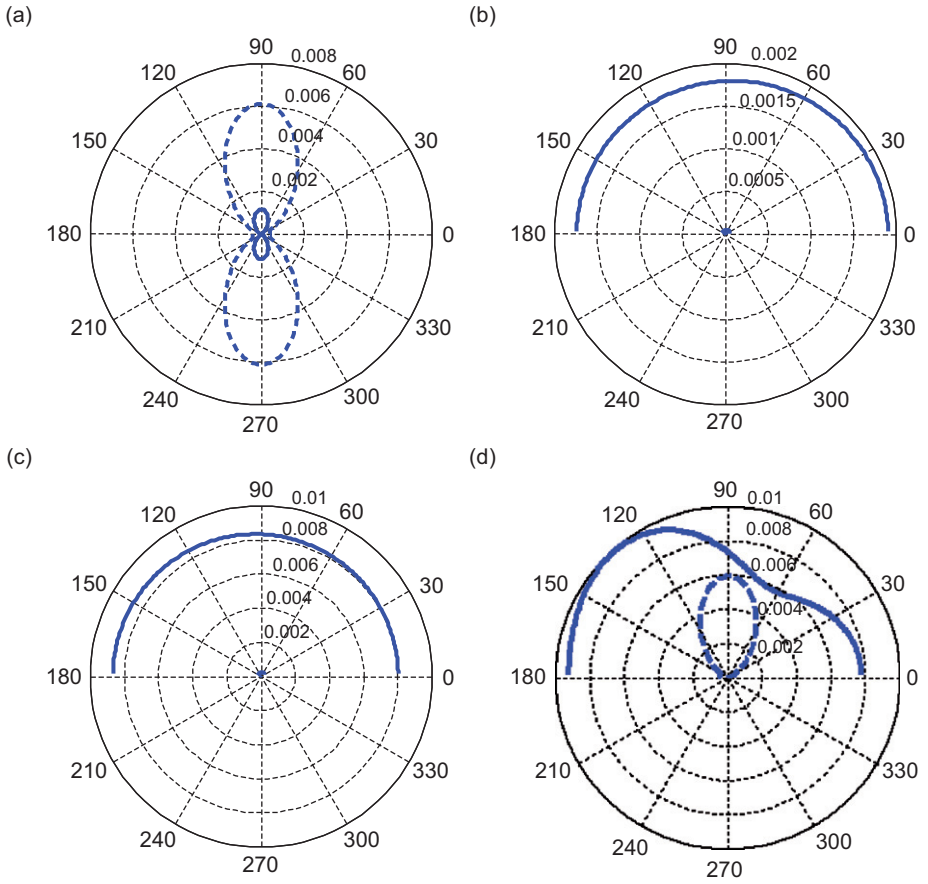

Fig. 15. Radiated pressure of large diameter hull at first axial mode by minimizing the sum of the axial displacement of the rigid end plates.

With this new boundary condition, Eq. (4.3) is used to replace Eq. (4.2) to evaluate the amplitudes A_1 and A_2 (see Eqs. (5) and (6) in Section 2.2). Only the results for the first axial mode of the two submarine hull models are shown to illustrate the effect of using a different end condition on reducing radiated pressure.

Figs. 17(a and b) show the controlled and uncontrolled radiated pressure of the conical shell and the total pressure of the small submarine, respectively. Figs. 18(a and b) show the corresponding results of the large submarine. The results of the radiated pressure for the cylindrical shell and hemispherical shell are not shown as they are the same as those shown in Figs. 6 and 10.

From Figs. 17(a) and 6(c), it can be seen that the radiated pressure of the conical shell for the small submarine model is drastically reduced by applying a radial constraint to the tail of the cone. Similar results can be observed for the large submarine model (see Figs. 18(a) and 10(c)). With the radial constraint, the radiated pressure of the conical shell is small compared with the cylindrical shell and hemispherical shell and it has a direct impact on the optimization of total radiated pressure.

Fig. 17(b) shows the controlled and uncontrolled radiated pressure of the small diameter hull. It can be seen that the control action is less effective with the constrained conical shell since the optimization process favors the broadside at the expense of on-axis radiation. The large diameter hull shows a more promising result (see Fig. 18(b)) with over 45% reduction in the on-axis radiated pressure.

6. General discussion

Results for the two submarine models shown in Sections 5.1–5.3 of this paper represent the modal radiation of typical medium to large conventional submarines subjected to an axial excitation. Unlike the previous study

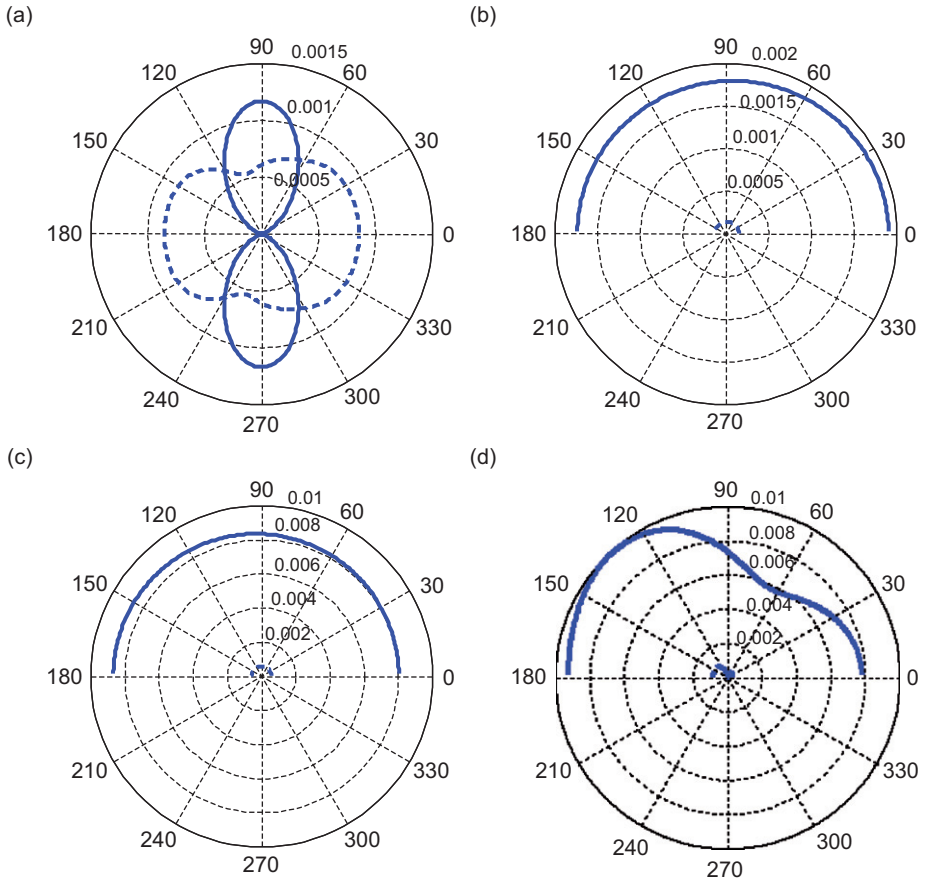

Fig. 16. Radiated pressure of large diameter hull at first axial mode by minimizing the total radiated sound power of the submarine hull.

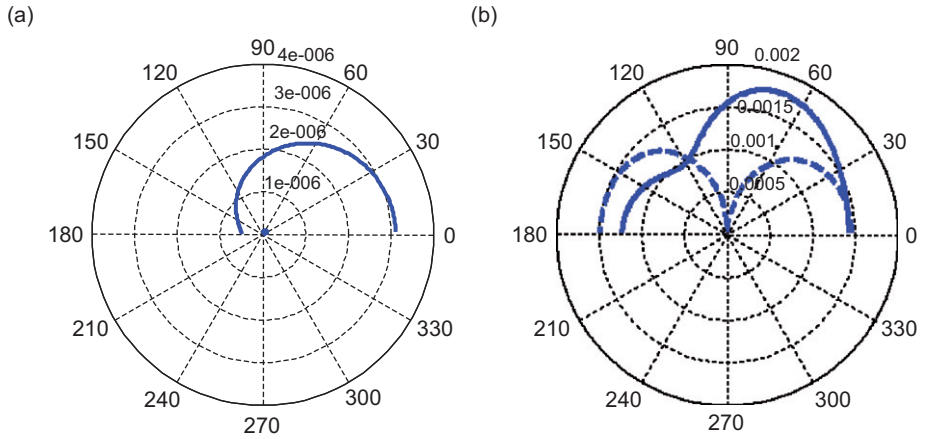

Fig. 17. Radiated pressure of small diameter hull with constrained conical shell at first axial mode by minimizing cylinder sound power: (a) due to conical shell; (b) total radiated pressure.

[7] where the submarine hull was modelled as a finite cylinder with rigid end plates, the effects of free-flooded end casings are considered here. Due to the free-flooding nature of the casings, they are typically more flexible than the main pressure hull and thus have a significant effect on the radiated pressure. Furthermore, it was found in Section 5.4 that the high contribution to far field radiation of the conical shell is attributed to the

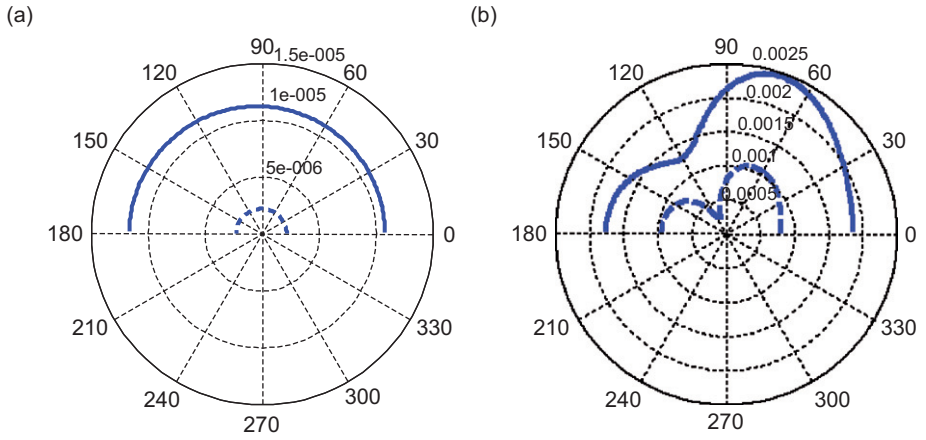

Fig. 18. Radiated pressure of large diameter hull with constrained conical shell at first axial mode by minimizing cylinder sound power: (a) due to conical shell; (b) total radiated pressure.

choice of boundary conditions. Hence an accurate modelling of the boundary condition is essential to the prediction of sound radiation and the assessment of the effectiveness of active control strategies.

7. Conclusions

An active control strategy is developed for the modal control of radiated noise from a submarine hull.

The study shows that the radiated pressure may be reduced by approximately 40–90% for the first three axial modes using active control moments for both submarine models with a free boundary condition at the end of the conical shell, and slightly less reduction with a constrained conical tail end. The amplitudes of the control moments are small compared with the excitation force and may be implemented by a series of PZT stack actuators through a circumferential stiffener.

The examples used in this study indicate that the contributions to the total radiated pressure of the submarine hulls are partially attributed to the choice of boundary conditions of the conical shell. It is therefore reasonable to suggest that, in addition to the application of active control techniques (an example of which is outlined in this paper), careful design and optimization of the end casings are effective means to reduce the radiated noise of a submarine.

The use of different cost functions for minimizing the radiated pressure has been examined briefly in this paper. It is shown that the radiated cylinder sound power may be used effectively as the cost function for minimizing the radiated pressure. The control strategy may be implemented by a number of accelerometers to measure the cylinder response.

Appendix A. The radiation of sound from the hemispherical shell

From the radial displacement of the hemispherical shell, one can formulate the expression for the pressure field based on the Helmholtz integral equation. However, in order to combine the radiated sound pressure of the hemispherical shell with the pressure hull, a semi-infinite cylindrical baffle should be attached to the hemispherical shell for the evaluation of pressure radiation (see Fig. A.1). As this combined hemisphere/cylinder structure is difficult to solve analytically, a hemispherical instead of cylindrical baffle is used in the present study.

For a hemispherical shell with a radial displacement $w_{\mathrm{hem}}(\theta)$ and backed by a hemispherical baffle, the far field radiated pressure is given by Wang et al. [12]:

$$p_{\mathrm{hem}}(R,\theta)=\frac{\omega^2\rho_f}{2k_f}\sum_{n=0}^{\infty}\left\{(2n+1)P_n(\cos\,\theta)\frac{h_n(k_fR-(L/2)k_f\,\cos\,\theta)}{h_n'(k_fa)}\right.$$
$$\left.\times\int_0^{\pi/2}P(\cos\,\theta_{\mathrm{hem}})w_{\mathrm{hem}}(\theta)\sin\,\theta\,\mathrm{d}\theta\right\}. \tag{A.1}$$

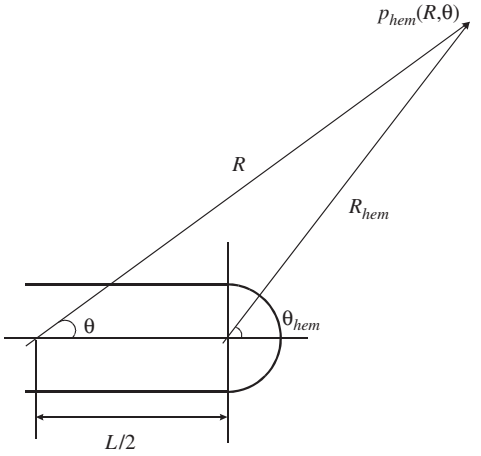

Fig. A.1. Far field noise radiated from the hemispherical shell showing the relationship between the observer and the center of the pressure hull.

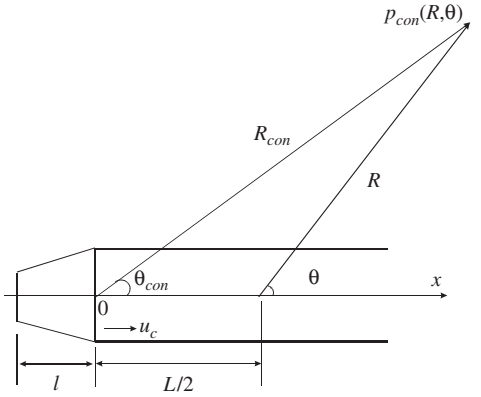

Fig. B.1. Far field noise radiated from the conical shell showing the relationship between the observer and the center of the pressure hull.

Note that the upper limit of integration in Eq. (A.1) is $\pi/2$ to represent the vibrating hemispherical shell. Also, to allow the radiated pressure of the hemispherical shell to be combined with that of the pressure hull, the distance between the center of the hemispherical shell to the observer R_{hem} has been replaced by $R–(L/2)\cos\theta$, and the meridian angle θ_{hem} replaced by θ (for $R_{\mathrm{hem}} \gg L/2$, see Fig. A.1). These transformations relate the radiated pressure of the hemispherical shell to the mid-section of the pressure hull. Eq. (A.1) may be solved by substitution of the radial displacement given by Eq. (3).

Appendix B. The radiation of sound from the conical shell

The evaluation of the far field noise radiated by the conical shell follows the approach adopted by Tso and Jenkins [1] where a conical element is approximated by a cylindrical element with the same volume displacement. Using this approach, the far field pressure radiated by a conical shell is given by Tso and Jenkins [1]:

$$p_{\mathrm{con}}(R,\theta) = \frac{\mathrm{j}\rho_f \omega^2 \mathrm{e}^{\mathrm{j}k_f R} \mathrm{e}^{\mathrm{j}k_f (L/2)\cos\theta}}{\pi k_f [R + (L/2)\cos\theta] \sin\theta \cos\alpha} \int_{-l}^{0} \frac{w_{\mathrm{con}} \mathrm{e}^{-\mathrm{j}k_f \cos\theta x}}{H_1(k_f r \sin\theta)} \,\mathrm{d}x. \tag{B.1}$$

Similar to Eq. (A.1), R_{con} has been replaced by $R+(L/2)\cos\theta$, and θ_{con} is approximated by θ (see Fig. B.1). Eq. (B.1) may be solved by substitution of the radial displacement given by Eq. (6).

References

[1] Y.K. Tso, C.J. Jenkins, Low frequency hull radiation noise. Report No. Dstl/TR05660, Defence Science and Technology Laboratory, UK, 2003.
[2] X. Pan, C.H. Hansen, Active control of vibration transmission in a cylindrical shell, *Journal of Sound and Vibration* 203 (1997) 409–433.
[3] X. Pan, C.H. Hansen, An experimental study of active control of vibration transmission in a cylindrical shell. *Proceedings of the 131st Meeting of the Acoustic Society of America*, Indianapolis, USA, 1996.
[4] A.J. Young, Active Control of Vibration in Stiffened Structures. PhD Thesis, University of Adelaide, 1995 156–234.
[5] Y.K. Tso, N. Kessissoglou, C. Norwood, Active control of a fluid-loaded cylindrical shell, part 1: dynamics of the physical system. *Proceedings of the Eighth Western Pacific Acoustics Conference*, Melbourne, Australia, 2003.
[6] N. Kessissoglou, Y.K. Tso, C. Norwood, Active control of a fluid-loaded cylindrical shell, part 2: active modal control. *Proceedings of the Eighth Western Pacific Acoustics Conference*, Melbourne, Australia, 2003.
[7] X. Pan, Y. Tso, R. Juniper, Active control of low frequency hull radiated noise. *Journal of Sound and Vibration*, submitted.
[8] S. Merz, S. Oberst, P. Dylejko, N. Kessissoglou, Y. Tso, S. Marburg, Development of coupled FE/BE models to investigate the structural and acoustic responses of a submerged vessel, *Journal of Computational Acoustics* 1 (2007) 23–47.
[9] R. Kinns, L. Thompson, N. Kessissoglou, and Y.K. Tso, Hull vibration forces transmitted via the fluid and the shaft from a submarine propeller. *Proceedings of the Fifth International Conference on High Performance Marine Vehicles*, Australia, 2006.
[10] M.C. Junger, D. Feit, *Sound, Structures, and their Interaction*, MIT Press, Cambridge, MA, 1985.
[11] A.W. Leissa, *Vibration of Shells*, National Aeronautics and Space Administration, Washington, DC, 1973 1–184.
[12] J.T.S. Wang, C.W. Lin, W. Stadler, The axisymmetric response of cylindrical and hemispherical shells to time-dependent loading. NASA CR-572, 1966.
[13] A.H. Nayfeh, *Perturbation Methods*, Wiley, New York, 1973.